

Structural and Optical Prosperities of Nickel Doped Zinc Oxide Thin Films Grown by Low Cost Modified SILAR Method

M. Karunakaran^{1,*}, R. Chandramohan², S. Balamurali², S. Gomathi², K. Kabila³ and T. Mahalingam⁴

¹Department of Physics, Sethupathy Govt. Arts College, Ramanathapuram – 623 502, India

²Department of Physics, Sree Sevugan Annamalai College, Devakottai - 630 303, India

³Department of Physics, Modern Arts and Science College, Jayankondam – 621 802, India

⁴Department of Physics, Karunya University, Coimbatore – 641 114, India

E. mail: phy_karuna@yahoo.co.in

Received: 26 Dec. 2013, Revised: 20 Feb. 2014; Accepted: 23 Feb. 2014

Published online: 1 May 2014

Abstract: The effect of annealing in Ni doped Zinc oxide (ZnO) semiconductor thin films grown by a modified SILAR method is presented in this study. The XRD diffraction patterns reveal good crystalline quality without any appreciable changes from pure ZnO films and are genuinely polycrystalline with a hexagonal wurtzite structure. Scanning electron microscopic (SEM) investigation suggested that both the shape of the crystals and the texture of the films were highly influenced by the SILAR method. The SEM morphology shows the formation of vertical nanorods and interestingly, Ni doped ZnO shows fiber-like structures with good uniformity. These nano thin films are promising candidate for solar cells, photo detectors, and gas sensors.

Keywords: SILAR, Ni doped ZnO, Structural studies, Morphological studies, annealing effect.

1. INTRODUCTION

Nanocrystalline materials have attracted a wide attention due to their unique properties and immense potential application in nano device fabrication [1-4]. Zinc oxide (ZnO) has a direct wide band gap (3.4 eV at Room temperature), which is an n-type semiconductor. In ambient condition, ZnO has a stable hexagonal wurtzite structure with lattice spacing $a = 0.325$ nm and $c = 0.521$ nm and composed of a number of alternating planes with tetrahedral-coordinated O^{2-} and Zn^{2+} ions, stacked alternately along the c-axis. It has attracted intensive research effort for its unique properties and versatile applications in transparent electronics, ultraviolet (UV) light emitters [5, 6], piezoelectric devices [7,8], chemical sensors [9-11] and heterogeneous photo catalysts [12-14]. It has been proposed as a more promising UV emitting phosphor than GaN because of its larger exciton binding energy (60 meV) [15]. All these predominant properties make ZnO a great potential in the field of nanotechnology.

Various chemical methods have been developed to prepare nanoparticles of different materials of interest. ZnO nanoparticles can be prepared on a large scale at low cost by simple solution based method, such as chemical precipitation [16-18], sol-gel synthesis [19], and hydrothermal reaction [20, 21].

In this background, the purpose of this investigation is to study the influence of Ni doping on the physical properties of ZnO thin films. Successive Ionic Layer by Adsorption and Reaction (SILAR) is an excellent method for the fabrication of undoped and doped ZnO thin films [22-23]. In this study a modified SILAR method is used.

2. EXPERIMENTAL DETAILS

ZnO thin films were prepared using a modified SILAR technique involving double dip. The 'Ni' doping was carried out by adding the $NiSO_4$ salts in the solution bath at the proportion of Zn:Ni as 100 : 3, 5, 10 respectively. ZnO thin films were grown using a two-step modified SILAR using a solution comprising 0.1 M Zinc Sulphate (99% e-Merck), 0.2 M sodium hydroxide with a pH value of 9 ± 0.2 deposited at bath temperature of 90 °C under optimized condition. In a modified SILAR all the precursor solutions are taken in a single beaker. Before deposition, the glass substrates were cleaned in hot chromic acid followed by cleaning with an alkali and acetone. The well-cleaned substrates were immersed in the chemical bath for a known standardized time followed by immersion in hot water for the same time for hydrogenation. The process of solution dip (step 1) followed by hot water dipping (step 2) is repeated for known number of times. The cleaned substrate was

alternatively dipped for a predetermined period in sodium zincate bath and water bath kept at room temperature and near boiling point, respectively. The addition of MSO_4 in the ratio of Zn:M as 100 : 3, 5, 10, 15 respectively in the first dip solution leads to the formation of M doped zinc oxide nano thin films where 'M' stands for Nickel here. The ZnO thin film formed was confirmed by XRD (RigakuUltima III) analysis and the micro structural analyses of the samples were performed using SEM (JEOL Model JSM - 6390LV).

3. RESULTS AND DISCUSSION

Figure 1 shows the typical X-ray diffraction pattern obtained for the Ni doped ZnO thin films grown using SILAR method with various molar concentrations such as 5, 10 and 15mM. The grain sizes were estimated using Debye-Scherrer's formula (Hammad et al. 2009), $D = k\lambda / \beta \cos\theta$ Where k is the shaping factor which takes value from 0.89 to 0.94, ' λ ' is the wavelength of the $\text{Cu-K}\alpha$ line, ' β ' is the full width at half maxima (FWHM) in radians and ' θ ' is the Bragg's angle.

The ' d ' (interplanar spacing) values of the XRD reflections were compared with standard ' d ' values taken from JCPDS diffraction file (No. 89-0511). Good agreement between the observed and standard ' d ' values suggests that the material deposited is ZnO with hexagonal structure. The doping molar concentration of the films produces a considerable improvement in crystallinity, showing more intense and sharper XRD peaks. The predominant peak at 34.51° indicates that NZO thin film is preferentially oriented along (002) plane.

The lattice parameter values are $a = 3.249 \text{ \AA}$ and $c = 5.205 \text{ \AA}$. The sharpened X-ray line profile and higher intensity of (002) plane is observed at 5mM to 10mM of nickel sulphate concentration. There is no other new peak is observed in this molar concentration as shown in fig. 1 (b). The predominant peak orientation is shifted from (002) plane to (101) plane for NZO prepared with 15 mM nickel sulphate solutions. Also (002) and (100) plane peaks intensities are observed to be slightly suppressed due to the extent of doping. In thin films unlike the bulk the amount of Ni present in solutions need not be present in the resulting films. Hence doping and extent of doping has to be evaluated by the composition analysis and the changes in the microstructural information. No other typical peaks corresponding to Ni or NiO were present. It is indicated that no phase transformation has taken place with the Ni incorporation and the structure remains tact with minor modifications within the volume.

The larger full-width at half-maximum (FWHM) observed in films prepared with 5 mM nickel sulfate concentration shows that the crystallite size is in the range of 47 - 57

nm.

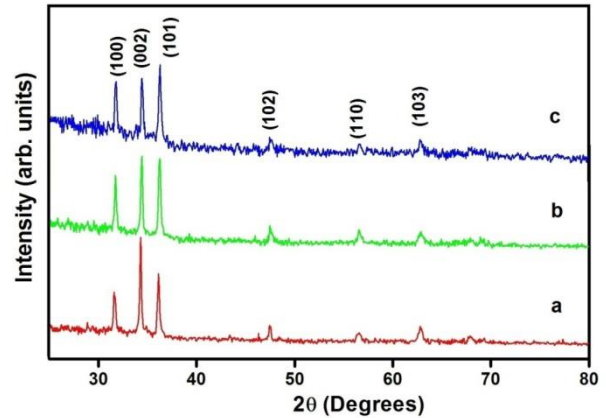


Fig. 1: XRD patterns of NZO thin films prepared at various molar concentrations such as (a) 5 mM (b) 10mM and (c) 15 mM

Table 1: Microstructural properties of various NiSO_4 concentrations prepared NZO thin films

Nickel sulphate concentrations (mM)	Crystallite size (nm)	Micro strain (ϵ)	Dislocation density $\delta \times 10^{15}$ lines/m ²	Stacking fault probability ($\alpha \times 10^{-4}$)
5	29.5	0.00167	1.14	0.12
10	44.6	0.00117	0.51	7.06
15	45.2	0.00115	0.48	11.0

range of 47 - 57 nm. Crystallite size of the film increase with doping concentrations. This may be due to Ni atoms being incorporated in the metallic sites or interstitials leading to NZO thin films. The micro strain (ϵ) was calculated from the slope of $\beta \cos\theta$ versus $\sin\theta$. Also it is observed that the micro strain value is depending on the crystallite size of the film. So that micro strain and dislocation density of the films decreases with increase of doping concentration. Due to the removal of defects in the lattice with increase in doping concentration of the micro strain in the films get released and attained a minimum value at 15mM of NiSO_4 . The doping concentration increases the predominant orientation angle shift towards higher angles and may be associated with increase of Ni atomic percentage in ZnO thin films. The stacking fault probability of the NZO thin films increases with doping molar concentrations. The NZO thin film with lower micro strain and dislocation density improves the stoichiometry of the films which in turn causes the volumetric expansion of thin films.

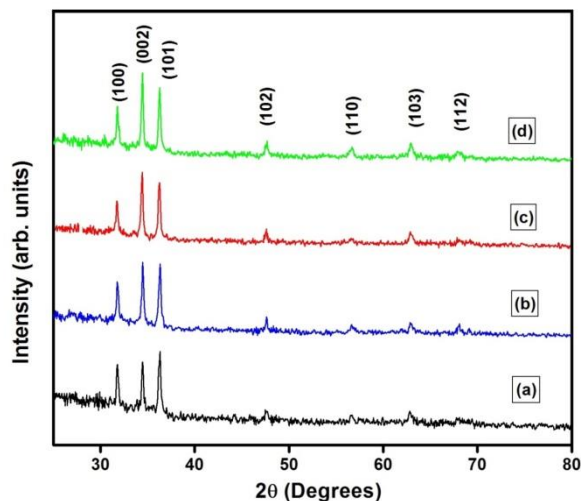


Fig. 2: XRD patterns of as-deposited and annealed NZO thin films (a) as-deposited (b) 200°C (c) 300°C and (d) 400°C

Annealing properties mainly affect the crystallinity of the film and also change the micro structural properties of the NZO films. Fig. 2 shows the X-ray diffraction patterns of Ni doped ZnO films with various annealing temperature such as 200, 300 and 400°C respectively together with unannealed samples. The annealed films were obtained by treating the samples at 200, 300 and 400°C for 60 min in air. Annealing produces a considerable improvement in crystallinity, showing more intense and sharper XRD peaks. The XRD patterns predict the increase of annealing temperature in the temperature range 0 to 400°C increasing the crystallinity and intensity. The predominant peak at 36.28° indicates that Ni doped ZnO thin film is preferentially oriented along the (101) plane. However, this preferential orientation tend to shift towards (002) orientation around 35.20° indicating a modification of the structure with annealing. The position of the predominant peak shift to higher angles for (110) and (002) plane at 300°C annealed film. All the diffraction peak intensities increase with increase of annealing temperatures. Also this same behavior has been observed at 400°C annealed film indicating that the optimized conditions for annealing be fixed between 300 and 400°C for further studies. The changes in the microstructure of the films with annealing are presented in Table 1.

Fig. 3 shows the typical SEM micrograph of as deposited ZnO, ZnO: Ni (15mM) and ZnO: Ni (annealed 400°C) respectively. All these films were grown at a pH 9 ± 0.2 . They show the presence of large, highly crystalline grains distributed uniformly. All micrographs show films with excellent uniformity and regularly stacked nanorods. Similar results were reported by our group [24].

Table 2: Micro structural properties of annealed NZO thin films

Annealing temperature	Crystallite size (nm)	Micro strain ($\epsilon \times 10^{-3}$)	Dislocation density ($\delta \times 10^{14}$)	Stacking fault probability ($\alpha \times 10^{-4}$)
As – deposited	45.2	1.15	4.44	11
200	48.2	1.12	3.57	5.47
300	49.7	1.05	2.00	1.81
400	52.8	0.88	1.42	1.57

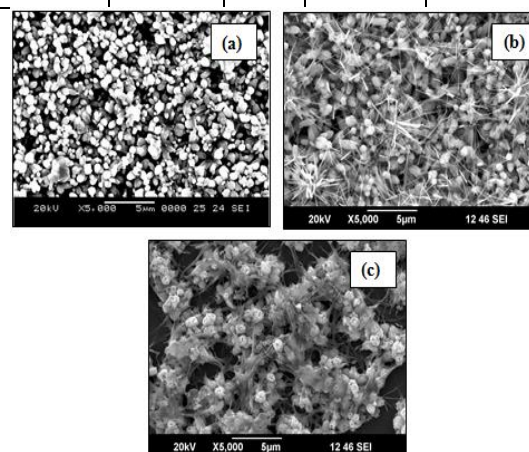


Figure 3: SEM micrograph of (a) undoped ZnO thin film prepared at 0.3 M ZnSO₄ (b) Ni doped ZnO thin film prepared at 15mM NiSO₄ (c) Ni doped ZnO thin film annealed at 400°C

The nanorods were found to be made of nanostructures with size between a few nanometers and 500 nm. From Fig. 3(a), it is observed that for the undoped ZnO films the nanorods are uniformly arranged without any stacked particles over the nanorods. While doping Ni with the ZnO matrix (Fig3 (b,c)), interestingly, nano fiber-like structures were formed throughout the stacked nanorods. It was originate that the average grain size (about 400 nm) vary with Ni incorporation, which is due to smaller radius of Ni²⁺ than that of Zn²⁺. The results are in good agreement with Qiu et al [25]. Annealing tends to gather these nano particles through the protruding nanofibres. This may be due to the excess energy available for agglomeration. It is clearly seen that the results are in good agreement with the results arrived from XRD studies.

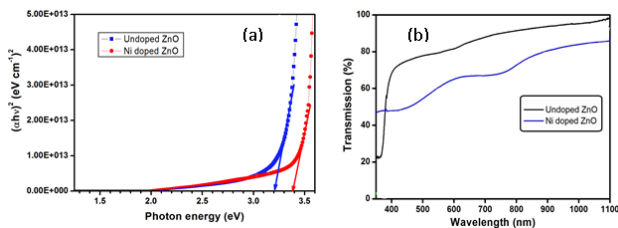


Figure 4: (a) Tauc's plot of undoped and Ni-doped ZnO thin films. (b) Optical transmission spectra of undoped and Ni-doped ZnO thin films

Figure 4 shows the transmittance spectra depict a high refractive index in the range of low absorption with a sharp fall of transmittance at the band edge implying the good crystal quality of the undoped and Ni-doped ZnO nanostructured films. High transmittance >90% is achieved at the far infrared region whereas the transmittance is found to decrease when ZnO films are doped with various metal content and the transmittance still decreases for all the cases. The undoped ZnO films show 70 to 80% optical transmission in the visible range. As it is clearly seen, the transparency of the films decreases when the dopants are added. The result is in good agreement with previously reported data [26]. The undoped ZnO film has a transmittance 74% in the blue region of the visible spectrum and the transmittance is found to have red shift. The decrease in optical transmission of NZO thin films can be due to the reduction in the grain boundaries. The slight reduction of transmittance is observed for the NZO films with Ni concentration 15mM. The decrease of transmittance with the wavelength is due to the decrease in band gap whereas transmittance is suppressed with increases of Ni content for the entire wavelength.

Table 3: Comparative optical parameters of undoped ZnO and NZO thin films

Film	Band gap (eV)	Extinction coefficient (k)	Refractive index (n)	Dielectric constant		Optical conductivity (s ⁻¹)
				Real part	Imaginary part	
Undoped ZnO	3.21	0.025	2.5	6.9	0.15	4.5 x 10 ¹³
NZO	3.39	0.031	2.9	5.4	0.34	4.4 x 10 ¹³

4. Conclusions

The structural and thickness properties investigations were performed for optimizing the film growth by chemical bath deposition employing double dip technique. It is observed that the films grown with

aqueous solutions are much better than that grown using non-aqueous solvents. The NZO thin films were prepared at various doping concentration such as 5, 10 and 15 mM of NiSO₄. The film thickness with respect to various doping concentration prepared NZO were observed. The structural and micro structural properties were discussed with doping concentrations prepared film. The predominant peak orientation was observed at (002) plane for lower doping concentration and (101) for higher doping concentration prepared NZO thin films. Also, the structural and corresponding micro structural properties were studied for various temperatures annealed NZO thin films. The higher doping concentration prepared NZO films were employed with post heat treatment at 200-400°C and micro structural properties were discussed.

REFERENCES

- [1] N. Golego, S.A. Studenikin and M. Cocivera, J. Electrochem. Soc., **147**, 1592 (2000).
- [2] Y. Lin, Z. Zhang, Z. Tang, F. Yuan and J. Li, Adv. Mater. Opt. Electron, **9**, 206 (1999).
- [3] X. Wang, J. Song, J. Liu and Z.L. Wang, Science, **316**, 102 (2007).
- [4] K. Keren, R.S. Berman, E. Buchstab, U. Sivan, E. Braun, Science, **302**, 1380 (2003).
- [5] K. Nomura, H. Ohta, K. Ueda, T. Kamiya, M. Hirano, H. Hosono, Science, **300**, 1269 (2003).
- [6] T. Nakada, Y. Hirabayashi, T. Tokado, D. Ohmori, T. Mise, Sol. Energy, **77**, 739 (2004).
- [7] S. Y. Lee, E. S. Shim, H. S. Kang, S. S. Pang, J. S. Kang, Thin Solid Films, **437**, 31 (2005).
- [8] R. Könenkamp, R. C. Word, C. Schlegel, Appl. Phys. Lett., **85**, 6004 (2004).
- [9] S. T. Mckinstry, P. Murali, J. Electroceram., **12**, 7 (2004).
- [10] Z. L. Wang, X. Y. Kong, Y. Ding, P. Gao, W. L. Hughes, R. Yang, Y. Zhang, Adv. Funct. Mater., **14**, 943 (2004).
- [11] M. S. Wagh, L. A. Patil, T. Seth, D. P. Amalnerkar, Mater. Chem. Phys., **84**, 228 (2004).
- [12] Y. Ushio, M. Miyayama, and H. Yanagida, Sensor Actuat., B **17**, 221 (1994).
- [13] H. Harima, J. Phys. Condens. Matter., **16**, S5653 (2004).
- [14] S. J. Pearton, W. H. Heo, M. Ivill, D. P. Norton, and T. Steiner, Semicond. Sci. Technol., **19**, R59 (2004).
- [15] M.A. Garcia, J.M. Merino, E.F. Pineda, A.J. Quesada, D. Venta, M.L.R. Gonza, G.R. Castro, P. Crespo, J. Llopis, J.M.G. Calbet, A.Hernando, Nano letter., **7**, 1489-1494 (2007).
- [16] Q.P. Zhong, E. Matijevic, J.Mater. Chem., **3**, 443 (1996).
- [17] W. Lingna, M. Mamoun, J.Mater. Chem., **9**, 2871 (1999).
- [18] D.W. Bhnemann, C. Kormann, M. R. Hoffmann, J.Phys. Chem., **91**, 3789 (1987).
- [19] Z. Hui, Y.Deren, M. Xiangyang, J.Yujie, X. Jin, Nanotechnology., **15**, 622 (2004).
- [20] J.Zhang, L. D. Sun, J.L. Yin, Chem.Mater., **14**, 4172 (2002).
- [21] W.J. Li, E.W. Shi, Z.W. Yin, J.Mater.Sci.Lett., **20**, 1381 (2001).
- [22] T.A.Vijayan, R.Chandramohan, S.Valanarasu, J.Thirumalai and S.P.Subramanian, J.Mater.Sci. **43**, 776 (2008).
- [23] T.A.Vijayan, R.Chandramohan, S.Valanarasu, J.Thirumalai, S.Venkateswaran, T.Mahalingam and S.R.Srikumar, Sci. Technol.Adv.Mater., **9**, 035007 (2008).
- [24] K Saravanakumar, K Ravichandran, R Chandramohan, S Gobalakrishnan, Murthy Chavali, Superlattices and

Microstructures, Volume 52, Issue 3, September 2012, Pages 528–540.

- [25] Qiu D J, Wu H Z, Feng A M, Lao Y F, Chen N B and Xu T N, *Appl. Surf. Sci.* **222**, 263, (2004).
- [26] D.Raviendra and J. K. Sharma, *J. Appl. Phys.*, 56, 641(1965).